# Enhancement in the design of Biometric Identification System based on Photoplethysmography data

Girish Rao Salanke N S
Research Scholar, Dept of SCSE.
VIT University, Chennai Campus,
Chennai, India – 600048
girishraosalanke@gmail.com

Dr. Andrews Samraj
Director,
Advance Science & Technology Research Center,
Salem, India - 636001
andrewsmalacca@gmail.com

Dr. Maheswari N
Associate Professor, Dept of SCSE
VIT University, Chennai Campus,
Chennia,India-600048
maheswari.n@vit.ac.in

S.Sadhasivam
Asst.Professor, Mahendra Engineering College,
Tiruchengode, India.
sivam.sadha@gmail.com

***Abstract* - In the recent years, automated security systems have become one of the major concerns. Secure and reliable authentication of a person is in great demand. In this paper, we propose the applicability of Photoplethysmograph (PPG) signal for human identification. Fourier series analysis and Semi Discrete Decomposition methods are applied to extract the features that appear to offer excellent discrimination among subjects. The main obstacle while analysing a PPG signal is the presence of noise, contaminated by motion artifact. The proposed method exhibits good identification accuracies not just with the normal PPG signals, but also with the motion artifact PPG signal.**

***Keywords - Photoplethysmograph (PPG), Motion Artifact, Fourier series Analysis, Semi Discrete Decomposition (SDD), Biometrics.***

## I. INTRODUCTION

Biometrics is a science of identifying a person using his physiological and/or behavioural characteristics[1]. Traditional biometrics like fingerprint[4], palmprint[13], face[8] and iris[5] have common weakness in their vulnerability to spoofing and even some of the other traits can be used if the person is dead. Such problems can be solved using signals like EEG[9], ECG[11] and PPG[2]. PPG signals have been used extensively in clinical diagnosis for many years. It has been recently suggested by the research communities that PPG signal can also be used as a biometric for human identification recognition. Most of the PPG biometrics work reported earlier [6][14]assumed that the PPG signal is free from motion artifact.

In most environments the PPG signal is contaminated by motion artifact and surrounding light variation luring recordings. Changes in surrounding light can be rejected using the emission of modulation of signals from an infrared emitter. The most troublesome problem with PPG signal while developing an authentication system is the motion artifact. These artifacts arise mainly as a result of the air gap between the sensor and the skin which leads to poor estimation of physiological parameters from the recording. Motion artifact is mainly low frequency interference and it is random in nature. Even a slight movement by the subject while recording would then invariably disturb the contact between the sensor and the subject's body, corresponding the PPG signal obtained during such periods to be corrupt with motion artifacts.

The rest of this paper is organized as follows: Section 2 deals with theoretical framework and section 3 presents the methodology. Section 4 presents the results & discussion. Finally, Section 5 contains the conclusion.

## II. THEORETICAL FRAMEWORK

### *A. Fundamentals of PPG Signal*

PPG signals provide a non-invasive and accurate methodology to obtain valuable physiological information such as blood oxygen saturation, heart rate and blood flow.

The blood in human body is being pumped from the heart to all parts in the body by blood vessels called arteries. Blood pressure is the force of blood pushing against the walls of the arteries. Each time the heart beats it pumps out a considerable volume of blood to the arteries. Systolic pressure which is the highest blood pressure occurs when heart is in pumping motion. Diastolic pressure is lowest blood pressure when heart is in resting[7].Since blood pressures are an indirect measurement of heart beats and the blood pressure tends to change according to the time and emotion. For instance, blood pressure will rise when a subject is awaken and excited. The unit for measurement of blood pressure is in mmHg and the notation will be systolic followed by diastolic pressure. The Photoplethysmograph (PPG) signals reflect the change in blood volume caused by blood vessel expansion and contraction, which can be detected by photodiode if external light is illuminated into tissue. This method is based on the idea that if an external applied pressure in the cuff is equal to the arterial pressure instantaneously, the arterial walls will be unloaded (zero transmural pressure) and the arteries will not change in size. In this condition, the blood volume will not change.

The Photoplethysmographic sensor used to read a PPG signal has an infrared emitter and photodiode detector. The intensity of light from infrared emitter which reaches the photodiode detector in either reflection or transmission will be measured to determine the blood volume changes. The Photoplethysmographic sensor will be placed below the tip of the finger and pressure will be applied on the proximal phalanx. Since the cuff is wrapped on the proximal phalanx of the finger rather than arm, it makes less discomfort for prolonged use. The blood volume changes on the finger will be notified by the sensor and transmitted to the system by wired or bluetooth transmitter. There will be a timer attached on the device to time the cuff pressure applied time and transmitter so that it is semi-continuous measurement. This is because to decrease the energy consumption of Bluetooth transmission and to avoid discomfort of the subject's finger due to continuous pressure applied.

The idea of the blood pressure sensor is much like the Photoplethysmograph Fingernail Sensor for measurement of finger force which is mentioned by Stephen A. Mascaro and H. Harry Asada [14]. The finger force is measuring colouration of fingernail by using reflectance Photoplethysmography. A sample PPG signal waveform extracted from the above Finger nail sensor under normal condition is shown in Figure 1 .

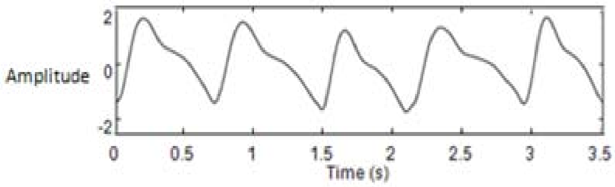


Figure 1. A Sample PPG Waveform

*B. Fourier Series Analysis*

A periodic function **f(t)** can be represented by an infinite sum of sine and/or cosine functions that are harmonically related. That is, the frequency of any trigonometric term in the infinite series is an integral multiple, or harmonic, of the fundamental frequency of the periodic function[10]. Thus, given f(t) is periodic (e.g. square wave, triangular wave, half rectified wave,etc.), then f(t) can be represented as follows:

$$f(t) = a_0 + \sum_{k=1}^{\infty}[a_k \cos(k\omega_0 t) + b_k \sin(k\omega_0 t)] \tag{1}$$

where k is the integer sequence 1,2,3,..........∞

$a_0$,$a_k$ and $b_k$ are called the Fourier coefficients, and are calculated from f(t),$\omega_0 = 2\pi/T$ is the fundamental frequency of the periodic function f(t) with period T, and $k\omega_0$ is known as k-th harmonic of f(t).

$a_0$,$a_k$ and $b_k$ can be calculated as follows

$$a_0 = \frac{1}{T}\int_{t_0}^{t_0+T} f(t)dt \tag{2}$$

$$a_k = \frac{2}{T}\int_{t0}^{t0+T} f(t)dt\ cos(k\omega_0 t)dt \tag{3}$$

$$b_k = \frac{2}{T}\int_{t0}^{t0+T} f(t)dt\ sin(k\omega_0 t)dt \tag{4}$$

The Pre-processing section to be used in methodology uses the above mentioned method to reconstruct the original PPG signal from the contaminated PPG signal based on a cycle to cycle basis.

*C. Semi Discrete Decomposition*

Dimension reduction refers to the process of taking a data-set with a number of dimensions, and then creating a new data-set with a fewer number of dimensions, which are meant to capture only those dimensions that are in some sense important. The idea here is that we want to preserve as much structure of data as possible, while reducing the number of dimensions it possesses; therefore we are creating a lower dimensional approximation of data.

We have used Semi Discrete Decomposition (SDD) algorithm for reducing the dimensions. The primary advantage of SDD approximations over other types of matrix approximations such as SVD is that it typically provides a more accurate approximation for far less storage. The SDD approximation of an *m* x *n* matrix *A* is a decomposition of the form

$$A_k = \underbrace{[\ x_1 x_2 \ \cdots \ x_k\ ]}_{X_k} \underbrace{\begin{bmatrix} d_1 & 0 & \cdots & 0 \\ 0 & d_2 & \cdots & 0 \\ \vdots & \vdots & \ddots & \vdots \\ 0 & 0 & \cdots & d_k \end{bmatrix}}_{D_k} \underbrace{\begin{bmatrix} y_1^T \\ y_2^T \\ \vdots \\ y_k^T \end{bmatrix}}_{Y_k^T} = \sum_{i=1}^{k} d_i x_i y_i^T. \tag{5}$$

Here each $x_i$ is an *m*-vector with entries from the set δ = { -1 , 0,+1 }, each $y_i$ is an *n*-vector with the entries from the set δ , and each $d_i$ is a positive scalar. We call this a *k*-term SDD approximation.

## III. METHODOLOGY

*A. Experimental Setup*

PPG data from 8 different subjects were used in this study. The data were collected by Andrews Samraj and Shoel Sayeed[8] recorded at Multimedia University(MMU), Malaysia. The description of the data and the recording procedure are as follows. The PPG signals were recorded using a Pulse Oximetry module (from Dolphin Medical, Inc) that was connected to a computer using a data acquisition software and captured with a sampling frequency of 37 Hz[12] as shown in Figure 2 . The main purpose of sampling the signal at this particular frequency is to highlight that even at this lowest frequency it is possible to capture the signal features that augment the authentication process. Sampling at a higher frequency is very fine and accurate and may be considered later on further progress. A total of 8 healthy subjects participated in this study. All the 8 subjects selected were research scholars and the average age of the subjects was 34. Two PPG recordings (normal and contaminated) were obtained from each subject with duration of 30 seconds. Figure 3 and Figure 4 shows normal PPG signal and the contaminated PPG signal of one subject recorded during the enrolment procedure. The intention of recording motion artifact signal is to achieve more accuracy in the identification procedure. The contamination is due to the motion artifact, which was induced due to the movement of finger connected to the device while recording the PPG signal. The normal PPG signal which is free from the motion artifact is used for the training purpose and the motion artifact signal for the testing purpose after undergoing the pre-processing.

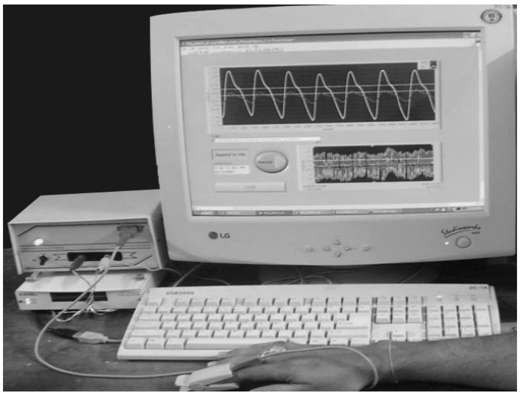

Figure 2. Experimental Set-up to record PPG signal

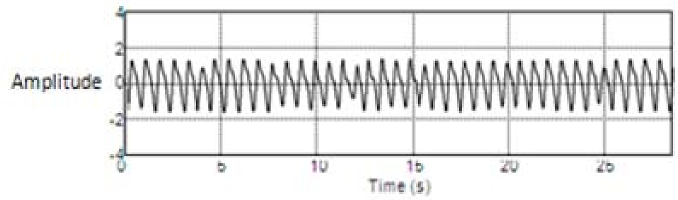


Figure 3. Normal (Artifact free) PPG Waveform

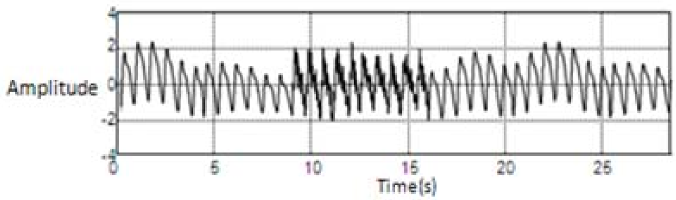


Figure 4 contaminated PPG Waveform due to motion artifact

*B. Data Pre-processing and Feature extraction*

The motion artifact PPG signal is pre-processed to remove the noise by Fourier series analysis. PPG cycle is represented by a reduced set of Fourier series coefficients $a_0$,$a_k$ and $b_k$. First a Each complete cycle of a PPG signal is identified and its time period, say T1 is identified as shown in Figure 5.

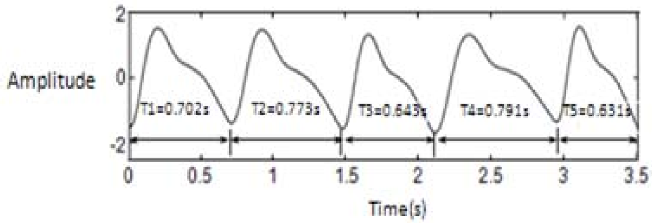


Figure 5. A Sample PPG Waveform considered for calculating Fourier Co-efficients

Assuming that its first cycle repeats itself endless by Fourier coefficients say ${}_1a_0,{}_1a_k,{}_1b_k$ where k = 1,2,3 ,......∞ are computed using equations 2, 3 and 4 respectively. The above coefficients are calculated only for first cycle. Once the Fourier coefficients applicable for the first cycle are computed and stored, the second cycle (with its time period T2) is then identified and subjected to Fourier series expansion and Fourier coefficients ${}_2a_0,{}_2a_k,{}_2b_k$ again applicable to that cycle are calculated. This above process is repeated foe every cycle and the $n^{th}$ cycle is represented by its coefficients.

${}_na_0,{}_na_k,{}_nb_k$ ; k= 1,2,3,……..,∞.

A reverse process is applied to reconstruct the PPG signal $f_R(t)$ from the stored set ofr thye coeffiecients cycle by cycle. The first cycle is reconstructed as

$$f_R(t) = {}_1a_0 + \sum_{k=1}^{\infty} a_k\,cos(k\omega_1 t) + {}_1b_k sin(k\omega_1 t)] \qquad (6)$$

*for t= 0 to $T_1$*

where $\omega_1 = 2\pi/T_1$

similarly the $n^{th}$ cycle is constructed as

$$f_R(t) = {}_na_0 + \sum_{k=1}^{\infty} a_k\,cos(k\omega_n t) + {}_nb_k sin(k\omega_1 t)] \qquad (7)$$

*for t=$T_{(n-1)}$ to $T_n$*

where $\omega_n = 2\pi/T_n$

Even though k in the above equations 6 and 7 ranges from 1 to ∞, for a practical purpose only a few significant terms need to be calculated, we have taken the max value ok k as 10. The first 10 significant Fourier coefficients of the 5 cycles for the PPG waveform of Figure 3 is shown in Table 1 and Table 2

TABLE 1. Fourier Co-efficient values (a)

| | cycle 1 | cycle 2 | cycle 3 | cycle 4 | cycle 5 |
|---|---|---|---|---|---|
| $a_0$ | 0.255 | 0061 | -0.243 | 0.019 | 0.225 |
| $a_1$ | -0.877 | -0.823 | -0.825 | -0.842 | -0.840 |
| $a_2$ | -0.588 | -0.577 | -0.576 | -0.580 | -0.580 |
| $a_4$ | -0.096 | -0.091 | -0.090 | -0.092 | -0.092 |
| $a_5$ | -0.028 | -0.025 | -0.025 | -0.026 | -0.026 |
| $a_6$ | -0.008 | -0.007 | -0.008 | -0.002 | -0.003 |
| $a_7$ | -0.001 | -0.000 | -0.000 | -0.001 | -0.001 |
| $a_8$ | -0.002 | -0.0001 | -0.001 | -0.002 | -0.001 |
| $a_9$ | -0.001 | -0.000 | -0.000 | -0.001 | -0.000 |
| $a_{10}$ | 0.000 | 0.000 | 0.000 | 0.000 | 0.000 |

TABLE 2. Fourier Co-efficient values(b)

| | cycle 1 | cycle 2 | cycle 3 | cycle 4 | cycle 5 |
|---|---|---|---|---|---|
| $b_0$ | 0.693 | 0.782 | 0.788 | 0.592 | 0.786 |
| $b_1$ | -0.026 | 0.021 | 0.018 | -0.063 | 0.018 |
| $b_2$ | -0.143 | -0.113 | -0.115 | -0.167 | -0.115 |
| $b_4$ | -0.046 | -0.026 | -0.023 | -0.026 | -0.025 |
| $b_5$ | -0.031 | -0.013 | -0.014 | -0.045 | -0.014 |
| $b_6$ | -0.008 | 0.007 | 0.006 | -0.019 | 0.005 |
| b7 | -0.007 | 0.005 | 0.004 | -0.017 | 0.004 |
| $b_8$ | -0.008 | 0.003 | 0.002 | -0.016 | 0.002 |
| $b_9$ | -0.004 | 0.006 | 0.005 | -0.011 | 0.005 |
| $b_{10}$ | -0.004 | 0.005 | 0.004 | -0.011 | 0.004 |

The values of Fourier coefficients of higher order ( k > 7) diminish drastically as shown in Table 1 and Table 2. Figure 6 shows the reconstructed PPG signal using the first 7 significant Fourier coefficients.

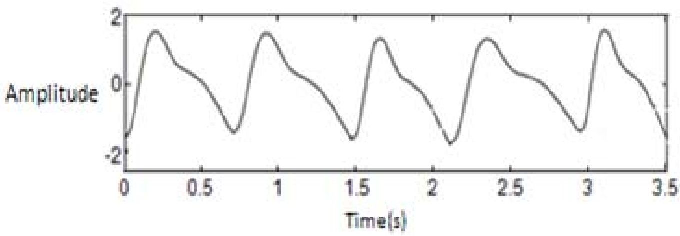


Figure 6. Reconstructed PPG Waveform from Fourier Co-efficients

When the subject moves while recording the signal, it results to contaminated signal. The contaminated signal say $f_c(t)$ will contain an additional component due to motion artifact. The contaminated signal can be represented as

$$f_c(t) = f(t) + f_a(t) \tag{8}$$

where f(t) is the original artifact free PPG signal and $f_a(t)$ is the motion artifact signal. Now Fourier series coefficients are calculated for the $n^{th}$ cycle of $f_c(t)$ by the following mentioned equations

$$ {}_n a_{0c} = \frac{1}{Tn}\int_0^{Tn} fc(t)dt = \frac{1}{Tn}\int_0^{Tn} f(t) + fa(t)dt = a_0 + \frac{1}{Tn}\int_0^{Tn} fa(t)dt \tag{9}$$

$$a_{kc}\frac{2}{Tn}\int_0^{Tn} fc(t)\cos(kw_n t)\,dt = {}_n a_k + \frac{2}{Tn}\int_0^{Tn} fa(t)\cos(kw_n t)\,dt \tag{10}$$

$${}_n b_{kc}\frac{2}{Tn}\int_0^{Tn} fc(t)\sin(kw_n t)\,dt = {}_n b_k + \frac{2}{Tn}\int_0^{Tn} fa(t)\sin(kw_n t)\,dt \tag{11}$$

Since a PPG signal has a very little correlation with the motion artifact signal, they can be assumed to be independent to each other. Hence the terms

$$\frac{2}{Tn}\int_0^{Tn} fa(t)\ \ cos(kw_n t)dt\ \ \&\ \ \frac{2}{Tn}\int_0^{Tn} fa(t) sin(kw_n t)dt$$

can be evaluated to be zero. Hence under this condition we will have

$${}_n a_{kc} = {}_n a_k \ \ \&\ {}_n b_{kc} = {}_n b_k \tag{12}$$

In general the motion artifacts are random in nature and can be assumed to have zero mean value. From equation 3.2.4, the artifact $f_a(t)$ has no DC value then ${}_n a_{0c} = {}_n a_0$. Thus by reconstructing the PPG signal from the computed Fourier series coefficients of the corrupted PPG signal, we obtain the error free PPG signal.

### *C. Feature Extraction & Selection Strategies*

Each recordings of the PPG signal, which is represented in the form of a matrix **A** is of order n by m, where n is the number of LED's and m is the number of sequential samples per unit time in our experiment n was fixed as 4 and m was taken up to 1 second. After applying SDD , matrix **A** can represented as follows

$$A = X_k D_k Y_k^T \tag{13}$$

where $X_k$ is *n x k* matrix , $D_k$ is *k x k* matrix and matrix and $Y_k^T$ is *k x m* matrix. Each row of X corresponds to a row of A and each column of $Y^T$ corresponds to a column of A. The diagonal entries of D, provides information about the importance of each of the components.

The actual average size of matrix A is (3,056). After the application of SDD the features are reduced to 764. Let ***F*** represents the feature vector. For computational reasons, it may be more efficient to remove several features at a time at the expense of classification accuracy. Depending on the requirements of the system complexity, two selection strategies can be adopted

#### *1. Strategy One*

The first ***p*** values of the sorted feature vector **F** were (used as features. Therefore the entire signal A is now represented by a highly discriminate feature vector of length ***F(P).*** These ***p*** largest values of **F** contain the feature component of each subject which can be used to discriminate from others. Throughout the experiment, to reduce the complexity of computation we set the value of $\boldsymbol{p}$ to be 5. Hence the reduced feature vector can now be represented as

$$F^1 = [a_1, \ldots\ldots\ldots\ldots, a_5] \tag{14}$$

2. *Strategy Two*

The first $\boldsymbol{q}$ components of **F** were used as features for matching purpose. The value of $\boldsymbol{q}$'s differ from subject to subject but finally when normalised, the values should result to uniqueness. Here the reduced feature vector can be represented as

$$F^2 = [a_1, \ldots, a_q] \tag{15}$$

$$i.e \sum_{i=1}^{p} F_i = 1 \tag{16}$$

So obtained feature vector $\boldsymbol{F^1}$ and $\boldsymbol{F^2}$ can be used further for matching and classification.

*D. Classification*

We first generate a matching score by the selected feature compared with the stored template. For each PPG signal, the Euclidean's distance is calculated and is compared with the set of samples stored in the system is computed. The template resulting in the smallest distance is considered to be the match. The Euclidean distance between two points x and y can be calculated as

$$\sqrt{(x-y)^2} = |x-y| \tag{17}$$

## IV. RESULTS & DISCUSSION

Figure 7 Shows the Euclidean's distance calculated between the referenced PPG data of a subject and eight other recordings of the same subject using the feature vector $\boldsymbol{F^1}$of the strategy one. Table 3 shows the results in terms of Euclidean's distance calculated between the referenced PPG data of a subject and eight other recordings of the same subject using the feature vector $\boldsymbol{F^2}$ of strategy two and the same is shown in Figure 8. On comparisons we clearly find that strategy two results in a better classification, where-in the intra subject variations are very less in terms for Euclidean's distance.

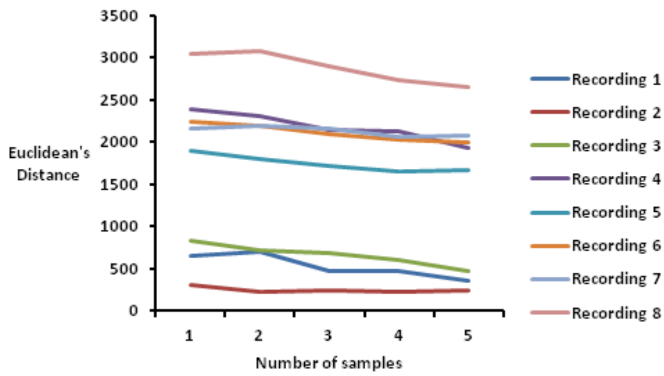


Figure 7. Intra subject Variations in terms of first feature vector $F^1$

TABLE 3 Intra Subject Variations in terms of Euclidean's distance using strategy two

| Recording1 | Recording2 | Recording3 | Recording4 | Recording5 | Recording6 | Recording7 | Recording8 |
|---|---|---|---|---|---|---|---|
| 646.44375 | 316.46375 | 838.09375 | 2396.994 | 1904.634 | 2235.444 | 2155.184 | 3050.984 |
| 706.84375 | 232.34375 | 719.47375 | 2310.044 | 1797.814 | 2200.844 | 2199.854 | 3079.304 |
| 470.3525 | 236.6025 | 679.9725 | 2140.133 | 1722.302 | 2097.063 | 2158.392 | 2904.322 |
| 473.83625 | 226.69625 | 595.67625 | 2121.106 | 1658.206 | 2028.896 | 2063.796 | 2742.706 |
| 360.2325 | 245.1125 | 479.2025 | 1939.433 | 1664.892 | 1997.703 | 2077.943 | 2651.943 |
| 302.09 | 40.15 | 475.23 | 1929.49 | 1528.75 | 1876.73 | 2078.98 | 2616.68 |
| 264.45 | 29.91 | 444 | 1909.9 | 1494.3 | 1861.53 | 2045.69 | 2603.84 |
| 158.59125 | 26.76125 | 416.08125 | 1898.861 | 1396.041 | 1751.051 | 2027.571 | 2479.071 |
| 163.88875 | 150.25125 | 383.43875 | 1797.639 | 1391.749 | 1744.579 | 1933.559 | 2483.009 |
| 154.9325 | 195.9775 | 356.4525 | 1749.853 | 1337.753 | 1728.513 | 1922.603 | 2449.443 |
| 71.28625 | 204.24375 | 308.86625 | 1710.896 | 1315.176 | 1698.246 | 1884.176 | 2443.106 |
| 98.24875 | 212.22125 | 327.64875 | 1702.999 | 1290.289 | 1716.749 | 1797.999 | 2395.169 |
| 94.71 | 251.07 | 280.58 | 1565.49 | 1227.46 | 1583.17 | 1725.32 | 2359.2 |

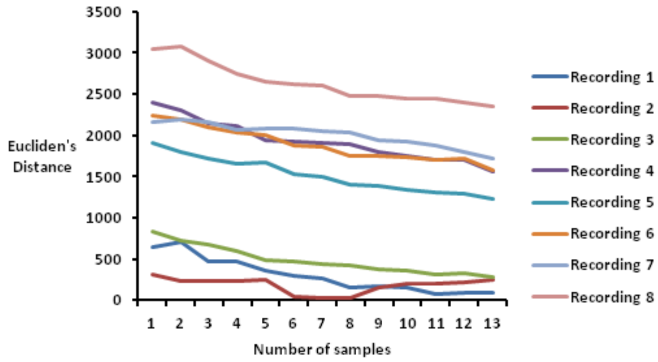


Figure 8. Intra Subject Variation in terms of normalisation considering Feature Vector $F^2$

Figure 9 and Figure 10 shows the Euclidean's distance between the referenced PPG of subject 1 with three different recordings of subject 2 using strategy one and strategy two as discussed earlier, here we can find a huge gap between their distances in the second strategy rather than the first strategy, this can be used as an improvement factor in using PPG signal as a biometric component in classifying individuals.

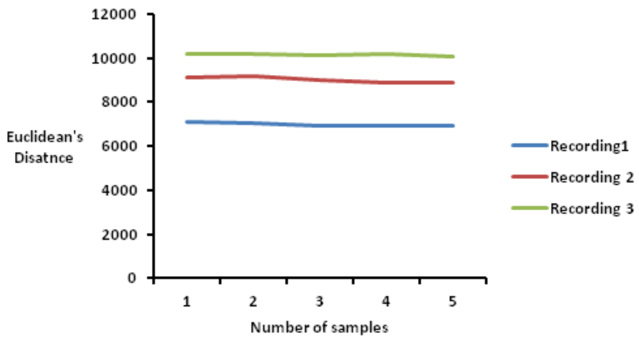


Figure 9. Inter subject variations using strategy two

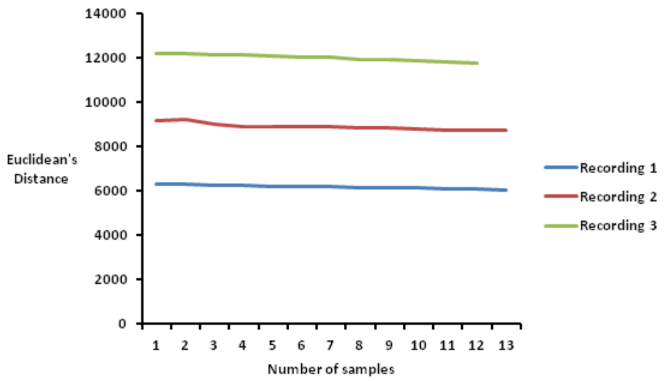


Figure 10. Inter subject variations using Strategy two

## V. CONCLUSION

In this paper, we have presented a novel approach to select the best set of features to efficiently identify individuals using PPG data. Our approach is based on relevant component normalisation from the feature vector. Experimental results show clearly the efficiency of this method.

## ACKNOWLEDGEMENT

The authors would like to acknowledge the permission to use the PPG data from Multimedia University, Malaysia.

## REFERENCES

[1]. A K Jain, A Ross and S Prabhakar, "An Introduction to Biometric Recognition", IEEE Trans. On Circuit Sys.14(1):4-20

[2]. Andrews Samraj, Shoel Sayeed, Loo Chu Kiong and Nikos E Mastorokis(2010)," Eliminating forgers based on intra trial varaiability in online signature verification using handgloves and photometric signals",In : Journal of Information security,Vol.1,23-28

[3]. C.M. Lee & Y.T Zhang,"Reduction of motion artifacts from photoplethysmographic recordings using a wavelet denoising approach," in *Proc. IEEE EMBS Asian-Pacific Conf. on Biomed. Engg.*, pp. 194-195, 20-22 Oct., 2003.

[4]. D Maltoni, D Maio, A K Jain and S Prabhakar , Handbook of Fingerprint Recognition, Springer 2003

[5]. Iris Recognition Technology http://www.argus-solutions.com/pdfs/irisrecogwilliams.

[6]. Jianchu yao, Xiodong Sun and Yongbo wan(2007)," A Pilot study on using derivatives of photoplethysmographic signals as a biometric identifier", In : Journal of engineering in medicine and biology society.

[7]. John Allen, "Photoplethysmography and its application in clinical physiological measurement", IOP Publishing, Phyiol, Meas, 28(2007)R1-R39.

[8]. J Lai, P Yuen, G Feng, "Face Recognition using Holistic Fourier Invariant Features", Pattern Recognition, 34(1),pp95-109,2001

[9]. Ramaswamy Palaniappan(2008), "Two-stage biometric authentication method using thought acitivity Brain Waves", In: Journal of Neural Systems,Vol.18,No.1,pp59-66.

[10]. R.N Bracewell." The Fourier transform and its applications", 3rd Edition,McGraw-Hill higher education,NY,2000.

[11]. T Y Wang, F Agrafioti, D Harzinakos, K N Plataniotis, "Analysis of Human Electrocardiogram(ECG) for Biometric Recognition.", EURASIP Journal on Advances in Signal Processing, Volume Article ID 14658,2008.

[12]. Waseem and Omer, "Microcontroller Design and Bluetooth signal Transmission for the Non-Invasive Health Monitoring System", In: EE B416 Electrical engineering Biomedical capstones(2009), Paper 17,P-29.

[13]. Watanabe, M., Endoh, T., Shiohara, M, and Sasaki, S., "Palm Vein Authentication Technology and Its Applications", In Biometric Consortium Conference, USA, 2005.

[14]. Y.Y Gu, Y.Zhang and Y.T Zhang (2003), " A Novel biometric approach in human identification by Photoplethysmographic Signals",In : Journal of information technology applications in biomedicine.